Journal of Inclusion Phenomena and Molecular Recognition in Chemistry **21**: 113–136, 1995.

Zeolite-Included Molecules Studied by NMR

CECIL DYBOWSKI

1. Introduction

Zeolites, like silicas and aluminas, are used widely in a variety of catalytic and noncatalytic applications in the chemical industry. To define the nature of processes occurring while molecules are absorbed, it is necessary to measure the properties of these absorbed molecules. Very frequently, the absorbed phases are neither liquid, gas, nor solid, being strongly influenced by the proximity of the zeolite structure. Aside, then, from the practical importance of these materials, the study of an unusual state of matter is yet another impetus for examining absorbed molecules. One may investigate these intermediate states in many ways, ranging from classical thermodynamic studies to sophisticated instrumental techniques, to define the structural and dynamic properties of absorbed molecules.

NMR spectroscopy has a particular strength in defining structural and dynamic properties of molecules, since NMR parameters depend strongly on the molecule's state. For example, the resonance position is sensitive to the local electronic environment, which changes with molecular conformation and with intermolecular arrangement. Dynamic parameters such as relaxation times are reporters of molecular internal and overall mobility. In addition, line widths of resonances can often be used to infer such useful information as the average distance from the location of one nuclear spin to another. Thus, NMR spectroscopy provides a sensitive spectroscopic tool with which to probe the absorbate's environment.

The information content of an NMR spectrum is quite specific [1]; however, because the technique is relatively insensitive, requiring substantial numbers of spins in the resonance region for a signal to be detected, its use is limited to the study of relatively high-surface-area materials loaded to reasonably high loadings [2]. In addition, since it is not inherently a surface tool, NMR spectroscopy may be subject to interferences, either from the material whose surface is being probed or from the spectrometer system. Therefore, most NMR spectroscopy has been performed on high-surface-area materials such as zeolites.

The extreme sensitivity of NMR parameters to slight differences in the local environment means that NMR spectra of molecules in contact with amorphous solids are often broadened by the distribution of structures and/or environments, with a concommitant loss of detail. Crystalline zeolites are generally rather homogeneous, and molecules absorbed in them can be expected to have NMR spectra of higher resolution than molecules in an amorphous material such as a silica-alumina. Hence, zeolites are ideal systems to be

investigated with NMR spectroscopy.

2. Effect of Exchange in NMR Spectroscopy

The principal effect of a surface is to provide sites for localization of an absorbed molecule. From the NMR standpoint, each site may be considered a unique state of the molecule with unique NMR parameters. If the molecule were localized at a site sufficiently long, one would detect only the NMR parameters of the molecule in that state. Because surfaces, and catalytic surfaces in particular, may not bind molecules strongly enough that residence times at a site are long on the NMR time scale (milliseconds to seconds), the detected signal may result from a molecule exchanging among various sites.

Exchange imparts interesting NMR properties to a system, which have been discussed in many elementary texts [3]. Here, I review simple concepts which, nevertheless, provide a useful framework for understanding the NMR spectroscopy of molecules absorbed in a catalyst such as a zeolite when exchange is present.

2.1 RAPID EXCHANGE AND CHEMICAL SHIFTS

In general, exchange can result in rather involved NMR results. In the limit that residence times are long and exchange rates are low, one detects individual resonances for molecules in all the various sites. In the range of intermediate exchange, the lineshapes can be rather complex, and will depend on the nature of the exchange. However, if exchange is rapid on the time scale of NMR interactions, the results are simple averages.

Consider the observed chemical shift of some nucleus on a molecule rapidly exchanging among several environments. Let the shift of the nuclear species be δ_i when it is localized for a long time on site i. Because of exchange between sites, one detects only an average chemical shift:

$$\delta = p_1\delta_1 + p_2\delta_2 + p_3\delta_3 + ... \quad (1)$$

where p_i is the probability of the molecule residing at site i. In cases in which only a few sites participate in exchange on the NMR time scale, one need only consider those sites in performing the average of Equation 1.

The problem of the effect of exchange between two sites on chemical shift is illustrative of the effects of adsorption on the detected NMR spectroscopy. In this case, the exchange may be represented by the following process:

$$A + S \underset{}{\overset{K}{\rightleftarrows}} S - A \quad (2)$$

where S is a vacant site, A is the unbound adsorbate, S-A is the complex formed by

adsorption, and K is the equilibrium constant for this exchange. As examples of systems where this model might be appropriate, one may cite the interaction of a molecule in the voids of the material with a specific adsorption site on the surface of the void space, and the interaction of a molecule from the bulk gas or liquid interacting with a site at a surface. Considering the total number of adsorption sites to be N^*, the total number of molecules to be N_0, and the equilibrium constant for the exchange process to be K, one can calculate the probability that the molecule is in the adsorbed state by Equation 3:

$$p_a = \frac{1}{2}\left(1 + \frac{N^*}{N_0} + \frac{1}{KN_0}\right) \pm \frac{1}{2}\left(\left(1 + \frac{N^*}{N_0} + \frac{1}{KN_0}\right)^2 - 4\,\frac{N^*}{N_0}\right)^{1/2} \qquad (3)$$

The probability that the molecule is not absorbed in this two-site case is $1 - p_a$. Using this result and Equation 1, one can predict the average chemical shift of the nuclear species as a function of N_0, the total concentration:

$$\delta = \delta_0 + (\delta_{ads} - \delta_0)p_a. \qquad (4)$$

In the limit that adsorption is strong or there are many adsorption sites [$KN^* >> 1$], Equation 4 simplifies to

$$p_a = \frac{N^*}{N_0} \qquad (5)$$

and so

$$\delta = \delta_0 + (\delta_{ads} - \delta_0)\left(\frac{N^*}{N_0}\right). \qquad (6)$$

The shift approaches that of the unabsorbed material as N_0 becomes very large. For the case that there are fewer molecules than there are adsorption sites, i.e., $N_0 << N^*$, the value of p_a approaches one. In this condition, one measures a seemingly coverage-independent chemical shift, which is the shift of the molecule while bound at the site.

It is important to note that some or all of the bulk gas phase may NOT be in rapid exchange with the sorbed material, in which case one detects a resonance for that material not participating in exchange at the unshifted position. N_0 is then the sum of material absorbed and that part of the bulk phase participating in exchange with the sorbed state, not the total amount including the material not in exchange. In many cases, the exchange may be between sites in the zeolite, perhaps one being a physisorption site and the other a more strongly bound site.

2.2 SPIN-LATTICE RELAXATION IN AN EXCHANGING SYSTEM

The spin-lattice relaxation rate is affected by exchange between sites. Considering two sites A and B, we let $x(t) = M_A(t) - M_A^0$ and $y(t) = M_B(t) - M_B^0$, where $M_i(t)$ represents the magnetization at site i and M_i^0 is the equilibrium magnetization at that site, one obtains the following two differential equations:

$$\left(\frac{dx}{dt}\right) = -K_A x + k_{AB} y \tag{7}$$

$$\left(\frac{dy}{dt}\right) = -K_B y + k_{BA} x \tag{8}$$

$$K_i = \frac{1}{T_{1i}} + k_{ij} \tag{9}$$

where k_{AB} is the rate constant for exchange from A to B, k_{BA} is the rate constant for the exchange from B to A and where i and j refer to the sites A and B. $1/T_{1i}$ is the intrinsic relaxation rate if the molecule remained at site i indefinitely. Equations 7 and 8 may be solved simultaneously to give solutions for x(t) and y(t):

$$x(t) = \exp(-\bar{\lambda}t)[X_1 e^{-\Delta t} + X_2 e^{\Delta t}] \tag{10}$$

$$y(t) = \exp(-\bar{\lambda}t)[Y_1 e^{-\Delta t} + Y_2 e^{\Delta t}] \tag{11}$$

$$\bar{\lambda} = \frac{K_A + K_B}{2} \tag{12}$$

$$\Delta = \left(\frac{K_A + K_B}{2}\right)\sqrt{1 + \frac{4k_{AB}k_{BA}}{(K_A - K_B)^2}} \tag{13}$$

$$Y_1 = \frac{k_+ y(0) - x(0)}{k_+ - k_-} \quad \text{and} \quad Y_2 = \frac{x(0) - k_- y(0)}{k_+ - k_-} \tag{14}$$

$$X_1 = k_- Y_1 \quad \text{and} \quad X_2 = k_+ Y_2 \tag{15}$$

and

$$k_\pm = \frac{K_B - \bar{\lambda} \pm \Delta}{k_{BA}} \,. \tag{16}$$

Understanding the NMR spectroscopy of absorbed species often hinges on

understanding the interchange of molecules among several adsorption sites. Thus, the theory of the effects of chemical exchange on line positions, line shapes, and relaxation parameters will be important in the analyses discussed below, because zeolites have various sites in which absorbed molecules may reside.

3. Xenon in Zeolites

3.1 GENERAL QUALITIES OF XENON NMR

Xenon gas has two stable isotopes that can be investigated with NMR spectroscopy: ^{129}Xe (26.4%) and ^{131}Xe (21.2%), having spins of 1/2 and 3/2, respectively. NMR spectroscopy of ^{129}Xe is relatively easy to perform. Owing to the adequate natural abundance (26.8%) and its magnetic moment, its receptivity relative to ^{13}C is 31.8. Thus, detection of resonant absorption in a sample of natural abundance is straightforward, neglecting differences in relaxation time and volume density. The resonance occurs at a frequency about 10% higher than ^{13}C at the same magnetic field strength; thus, experiments can be performed in a spectrometer designed for detection of the ^{13}C resonance by a slight change of the circuit tuning. ^{129}Xe in a variety of environments has been studied with NMR spectroscopy, and the range of shifts is over 5000 ppm [4], although the majority of shifts lie in a range of about 500 ppm. The dominant effect in ^{129}Xe-gas NMR is the strong dependence of parameters on gas density - the result of collisions experienced by xenon atoms. Owing to xenon's high polarizability, collisions affect the average chemical shielding due to the electrons. The resonance frequency of the gas at constant magnetic field, for example, changes dramatically with the density. It is this sensitivity to collisions and interactions with the local environment that has recently made the study of the ^{129}Xe NMR spectrum of the absorbed gas a topic of intense study in a number of laboratories.

The shift of the gas at infinitely low density is used as a reference against which shifts of xenon in other environments are reported; practical standard reference materials include xenon gas at various pressures and $XeOF_4$. The resonance of an isolated xenon atom has been estimated to be 5642 ppm more shielded (i.e., to lower frequency at constant magnetic field) than the bare xenon nucleus [5]. Similar calculations [6] for the isolated ^1H atom compared to the proton and ^{13}C relative to the bare ^{13}C nucleus give shifts of 18 ppm and 260 ppm, respectively.

The resonance shift of pure liquid xenon ranges between ~240 ppm at 160 K and ~160 ppm at 244 K, and the resonance of the pure solid occurs between ~270 ppm to ~305 ppm, depending on the temperature [7].

Gas-phase NMR spectra contain a great deal of information. In macroscopic spaces xenon-xenon collisions greatly exceed xenon-"wall" collisions. The ^{129}Xe resonance condition strongly depends on the gas pressure (or density). It becomes less shielded (shifts to higher frequency at constant magnetic field) the higher the gas pressure [8,9]. Over a reasonably wide range of density, the shift can be represented by a virial expansion:

$$\delta(T,\rho) = \delta_0 + \delta_1(T)\rho + \delta_2(T)\rho^2 + \delta_3(T)\rho^3 + \ldots\ldots \quad (17)$$

where $\delta(T,\rho)$ is the resonance shift at a temperature T and a density ρ, δ_0 is the resonance position at an infinitely low density, and $\{\delta_i(T)\}$ are the virial coefficients of the resonance shift in density [10]. The linear term results from binary collisions and the higher-order terms arise from collisions involving three- and four-body collisions. For densities below 100 amagats, terms with powers higher than 1 are essentially negligible. Over the wider range from 0 to 250 amagats [11], higher-order terms contribute and the virial coefficients have the following values for pure xenon gas:

$$\delta_1(298.15\ K) = 0.548\ (\pm 0.004)\ ppm/amagat$$
$$\delta_2(298.15\ K) = 1.69\ (\pm 0.2) \times 10^{-4}\ ppm/amagat^2$$
$$\delta_3(298.15\ K) = -1.63\ (\pm 0.1) \times 10^{-6}\ ppm/amagat^3$$

One can predict the magnitude of δ_1 by calculating the interaction of two xenon atoms during a binary collision [12]. The perturbation due to repulsive interactions between two xenon atoms giving a contribution to δ_1 of approximately 0.28 ppm/amagat at 298.15 K. The attractive part of the potential also contributes [11], but not to the extent it does for hydrogen or fluorine gas, for which the dominant effects on shift result from attractive interactions. The coefficients $\{\delta_i\}$ are temperature dependent [11]. The extrapolated shift, δ_0, of an isolated xenon atom is, however, rigorously temperature-independent [13]. This fact allows one to calibrate the temperature-dependent shifts of standard reference materials such as tetramethylsilane (TMS) [14]. The shift of the xenon resonance depends on the collision partner. For mixtures of xenon with other gases at sufficiently low densities, one may generalize to a multi-dimensional virial expansion of the shift, keeping only linear terms due to binary collisions:

$$\delta((T),\rho_{Xe},\rho_A) = \delta_0 + \delta_{1,Xe}(T)\rho_{Xe} + \delta_{1,A}(T)\rho_A \quad (18)$$

where $\delta_{1,i}$ is the second virial coefficient in the density of gas i [11]. Heteromolecular collisions are usually less effective in changing the xenon resonance position than are collisions with xenon atoms, the exceptions being paramagnetic species like O_2 and NO. The change in resonance position is due to bulk susceptibility and to a "contact-overlap" mechanism [15], in which Xe(5s) orbitals interact with π^* or π_g^* orbitals of the collision partner and unpaired electrons contact the xenon nucleus. Just as the second virial coefficient for xenon-xenon interactions is temperature dependent, so are the $\delta_{1,A}$ for interactions with other gas molecules [16].

Xenon, like many gases, dissolves to some extent in liquids [17]. The observed shifts tend to be independent of concentration, indicating the infinitely-dilute limit. In addition to bulk susceptibility, shifts in this limit are affected by specific or nonspecific interactions with solvent molecules. Specific interactions result from definite molecular associations, e.g., hydrogen bonding. Since xenon is relatively chemically unreactive, shifts are

attributable to specific interactions in only a few systems [18]. Non-specific interactions include: (1) magnetic anisotropy of the solvent molecule; (2) electric-dipole interactions; and (3) van der Waals interactions between the solute and solvent. Rummens [19] treated the contribution of the dispersive parts of the van der Waals interactions as if xenon were acted upon by a "reaction field" of a continuous medium arising from spontaneous electronic fluctuations in the solute, following the early work of Onsager [20] and Linder [21], giving a term in the medium shift proportional to $[(n^2 - 1)/(2n^2 - 1)]^2$, where n is the refractive index of the solution. The relation of the xenon shift to Rummens' function seems to hold for a rather diverse set of solvents, [17,18] as long as one considers sets of homologous materials, e.g., the linear alcohols. This is most probably because other contributions to the shift, including repulsive parts of the van der Waals interactions, are similar within an homologous series. Xenon dissolved in water shows an anomalously large shift when compared to similar materials, such as alcohols, probably because of a significant effect of local solvent structure. Similar interactions with the environment are seen in Ripmeester and Davidson's study [22] of enclathrated xenon, and in studies of polymer morphology through NMR of "dissolved" xenon [23,24].

3.2 XENON IN MICROSCOPIC SPACES

Obviously, the interaction of a xenon atom with its environment profoundly affects the observed NMR properties. In the macroscopic gas, the walls are sufficiently far apart that interactions with them are rendered statistically insignificant compared to interactions with other xenon atoms or other molecules. In solutions, the nature of the "solvent" seems to be the dominant factor, and the general trend is understood in terms of specific and nonspecific interactions with the solvent.

When one partitions the space in which xenon is confined by walls separated by dimensions of 0.5 to 10 nanometers, the interactions with the "walls" dominate, as is seen in the clathrates [25], in solution, and in intercalation compounds [26,27]. Zeolitic materials, of course, are paradigms of this effect. The regular crystalline structures formed by zeolite frameworks partition space into regions of molecular dimensions connected in regular arrays [28]. Xenon in such structures would be expected to have strong interactions with the zeolite, which should be clearly signaled in the NMR behavior. In addition to the manner in which space is partitioned microscopically, the presence of a framework bearing charge means that there also exist charge-compensating ions, with which xenon may interact. The amount and type of ion(s) associated with a zeolite have a significant effect on its catalytic and sorptive properties. Thus, it was proposed [29] that the NMR spectroscopy of absorbed xenon may detect features of the zeolite which are relevant to its catalytic properties such as where an ion resides, the kinds of coabsorbed materials, and the framework structure.

Figure 1 shows the adsorption isotherm, at 293 K, for xenon in Y zeolite containing both nickel and sodium counterions. The isotherm is approximately linear over the range. Because dehydrated Y zeolite has a typical pore volume of 0.34 cm^3/g [28], xenon

absorbed at 3 atoms per supercage corresponds to a density of 0.6 g/cm^3, a reasonably high density but quite a bit lower than the 3.5 g/cm^3 of liquid xenon [30]. Loadings in the range of 3 atoms per supercage correspond to equivalent densities in the range of 100 amagats.

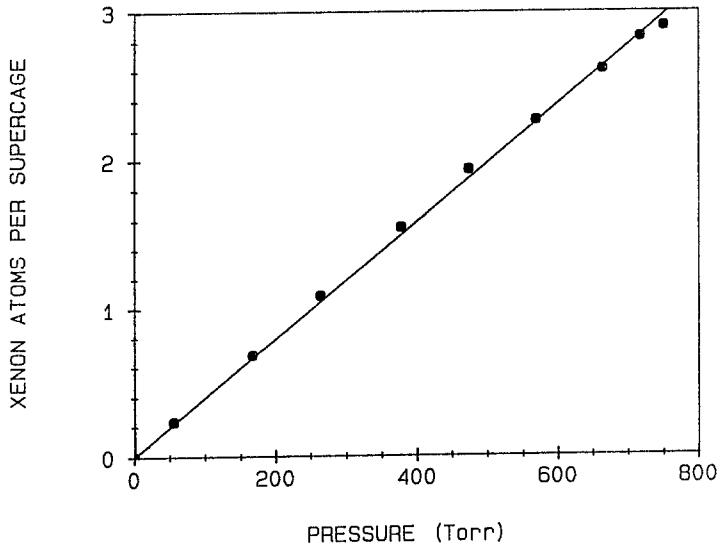

Figure 1. Isotherm for adsorption of xenon on a partially dehydrated Ni,Na-Y zeolite at 295 K. The solid line indicates the best fit to a linear isotherm for this material.

There are a number of interactions that contribute to the local environment of xenon in zeolites: (a) interaction with the "walls"; (b) interaction with other sorbed xenon atoms; (c) exchange among different adsorption sites; and (d) interaction with other absorbed material. In the absorbed state, the "walls" of the zeolite have a substantial effect on xenon. Ripmeester and Ratcliffe [31] describe a model in which two regimes are identified depending on the difference between the van der Waals radius of a xenon atom and the radius of curvature of the sphere formed by the substrate. Calculations based on the Xe-O Lennard-Jones potentials predict an optimum xenon-zeolite interaction of 20 kJ/mole in a hypothetical supercage with van der Waals radius of 12.5 Å. For zeolites with smaller cages (such as the α-cage of Na-A zeolite with a diameter of 11.5 Å) the adsorption potential for xenon has a single minimum at the center of the supercage (The energy at the minimum is 15 kJ/mole for Na-A zeolite). For zeolites with larger supercages (e.g, with a diameter of 14.5 Å), the adsorption potential for xenon has a minimum near the walls and a hump at the center of the supercage. (For Na-Y zeolite, the energy at the minimum is 15

kJ/mole at the wall with a barrier of 1.2 kJ/mole in the center.) In this model, the effect of the local environment depends on the ratio of the supercage volume to the surface area and divides into two classes: "clathrated" xenon in small supercages and "fluid" xenon in larger supercages.

Xenon diffuses through the interconnected supercages [32] and thus its NMR spectrum reflects the average of the local environments sampled during the free-induction decay of its nuclear magnetic signal. For a typical linewidth of 20 ppm in a magnetic field of 4.7 Tesla, the xenon free-induction decay persists for only a few milliseconds. The extent that the xenon diffuses during this time depends on the width and height of the potential barriers between adjacent adsorption sites and the occupancy of the sites. Consider the two classes of adsorption that emerge from the model of Ripmeester and Ratcliffe. For small supercages, adjacent minima are the centers of adjacent supercages and the potential barriers are at the windows. Assuming a barrier of 10 kJ/mole, a pre-exponential factor of $5x10^{-14}$ sec, and a loading of 1 xenon atom per 2 supercages, one calculates a site lifetime of $6x10^{-12}$ sec. A random walk in 1 msec would carry a xenon atom to many supercages. Thus, the time-averaged parameters (shifts, relaxation times, etc.) detected in an NMR experiment are averages over regions of rather large size (as compared to the supercage). Such averaging will tend to "wash out" the effects of inhomogeneities on smaller length scales, however, it should, in principle, be possible to detect large inhomogeneities with xenon NMR spectroscopy. An important result is that almost all xenon NMR information from such systems are exchanged-averaged quantities, of the sort one obtains from a simple theory as discussed in Section 2.

Such exchange-averaged quantities can then be considered to be a sum of contributions. Ito and Fraissard describe the NMR shift as arising from a series of terms, each the result of some interaction of xenon with the local environment:

$$\delta = \delta_{wall} + \delta_{xenon} + \delta_{adsorbate} + \delta_{electric} \qquad (19)$$

where δ is the observed shift, δ_{wall} is a contribution to the shift from collisions with the zeolite structure, δ_{xenon} is a contribution from other xenon atoms, $\delta_{adsorbate}$ arises from interactions with other adsorbates, and $\delta_{electric}$ is a contribution due to polarization of xenon by electric fields in the zeolite pore. Each of these terms depends on physical parameters of the system such as the density of xenon in the absorbed phase, the type, number and distribution of ions, and the temperature. As a first approximation, the first term is independent of xenon density. The second is given by an expansion in powers of the density, as for the gas. The third term is analogous to the contribution of other gases in a mixture and will depend linearly on the amount of co-absorbate. The contribution from electric fields, in this model, depends on factors such as the amount and positioning of ions; for systems like Na-Y zeolite at 295 K, it is considered to be negligible. Thus, for totally dehydrated Na-Y zeolite containing no other absorbates at 295 K, this model predicts that the shift depends on xenon density in the following manner:

$$\delta = \delta_{wall} + \delta_1\rho + \delta_2\rho^2 + \ldots\ldots\ldots \qquad (20)$$

where ρ is the density of absorbed xenon. If the isotherm is linear, then an analogous expression in the gas pressure at equilibrium can be used, as shown in Figure 2 for xenon in Na-Y zeolite [33]. The linearity of this plot and the virtual linearity of the isotherm over this range indicates that only the first two terms of Equation 20 make significant contributions to the ^{129}Xe NMR shift under these conditions. The intercept gives a value for δ_{wall} of 57.4 (±2) ppm; thus interactions with the framework do have a significant effect on the ^{129}Xe NMR properties. The parameter δ_1, when the density is expressed in amagats, has a value of 0.40 ppm/amagat, somewhat less than the value of 0.548 ppm/amagat observed for xenon in the bulk.

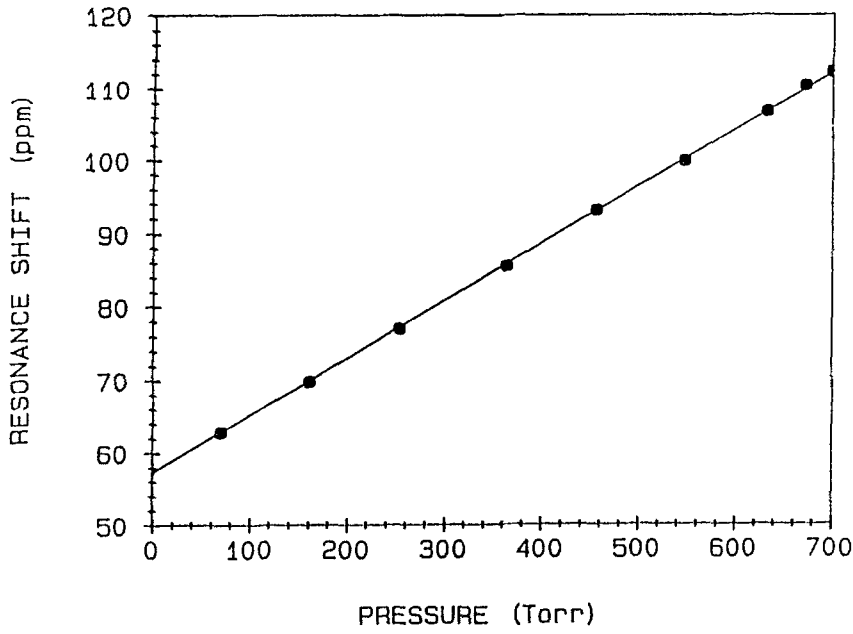

Figure 2. The dependence of ^{129}Xe NMR shift of xenon absorbed in a partially dehydrated Na-Y zeolite on pressure of the gas above the zeolite. The zero of the shift scale is the point extrapolated to P = 0 for bulk xenon by Jameson's equation (Equation 1).

Ito and Fraissard argue that this discrepancy results from restricted diffusion from one cage to another, effectively decreasing either the frequency or impact of xenon-xenon collisions, or both. If one assumes only collision frequency is altered by the presence of the zeolite (i.e., the zeolite merely acts as a steric hindrance to decrease the rate of xenon-xenon collisions but does not alter the microscopic details of the xenon-xenon collision), the ratio of these two parameters (0.73) is the relative number of collisions per unit time for

absorbed xenon compared to a bulk gas at the same number density. The fact that both δ_{wall} and δ_1 are the same for Na-Y zeolites of varying silicon/aluminum ratios [34] demonstrates that neither interactions with the wall nor xenon-xenon collisions are affected by the amount of aluminum and silicon in the framework of these materials. Thus, minor changes in structural parameters accompanying changes in silicon-to-aluminum ratio of Y zeolites are not sensed by this xenon NMR technique. Indeed, Ito and Fraissard found that the Na and H forms of Y zeolite were indistinguishable by xenon NMR spectroscopy, showing that interactions with these ions are also either negligible or the same for these conditions.

The dependence of ^{129}Xe NMR shift on the xenon density in the absorbed phase can be more complex than that of xenon in Na-Y zeolite at 295 K. For example, in their early work, Ito and Fraissard observed that the dependence of shift on xenon density in a calcium Y zeolite was distinctively curved, with a minimum shift at a loading of approximately 1.75 xenon atoms per supercage. Similarly, Scharpf et al. [33,34] found that a Y zeolite containing a mixture of nickel and sodium counter-ions exhibited a similar density dependence of the shift. Two, more thorough, studies [35,36] demonstrated that this behavior may be viewed as evidence for exchange of xenon between two different adsorption sites [37,38], and could therefore be modeled as an exchange-averaged shift as discussed in Section 2. The two sites could be, for example, a site near an ion (a chemisorption site) and a site in the pore volume of the supercage (a physisorption site). They might also be a site inside the zeolite particle and one in a gas phase outside the zeolite particle. They could be a site near the wall of the pore and one farther from the wall caused by steric or energetic variation of absorption within the pore [39]. Whatever the nature of the two sites, the shift when xenon is fixed at one site must be measureably different from that at the other, and there must be rapid exchange between the two sites on the NMR time scale. The average shift can be written as follows, by application of the exchange averaging discussed in Section 2:

$$\delta = \left[\frac{N_A}{N}\right]\delta_A + \left[\frac{N\text{-}N_A}{N}\right]\delta_B \tag{21}$$

where N_A is the equilibrium population of site A, and N is the total amount of material adsorbed on the two sites. If A is a site of limited sorption capacity such that $N >> N_A$, this result approximately becomes:

$$\delta = \delta_0 + \delta_1 N + \frac{[N_A \delta_A]}{N} \tag{22}$$

where δ_0 is a density-independent term and δ_A is a shift coefficient describing the effects of "sticky" collisions with the special sites. This mechanism predicts that, under some conditions, the average shift will vary inversely with N and linearly with N under other conditions. If δ_A and δ_1 are positive numbers, the minimum value of δ is reached for $N_{min} = [\delta_A N_A/\delta_1]^{1/2}$.

There is still the question of the identity of the sites. If site B is identified as a dense gas-like material in the pores of the zeolite, δ_B will depend on uptake (like the gas depends on density), giving a complex dependence of the shift on N. If interactions at site A (presumed to be at the wall or at ions) perturb the electronic structure of xenon, this mechanism could account for the observed effects in certain zeolites. Early work by Ito and Fraissard [34] demonstrated that replacement of sodium by calcium introduced this sort of term into the density dependence of the xenon NMR shift. Our work on xenon in Ni,Na-Y zeolites [35] with varying nickel contents showed that the strength of this term in the inverse of the uptake depends sharply on the nickel content of these catalysts and on the state of hydration of the ions. Shifts in fully hydrated samples show no evidence of a term inverse in the density. This can be most easily seen in a plot of δ_{-1} [$\equiv N_A\delta_A$] as a function of the amount of sodium replaced by nickel [Figure 3].

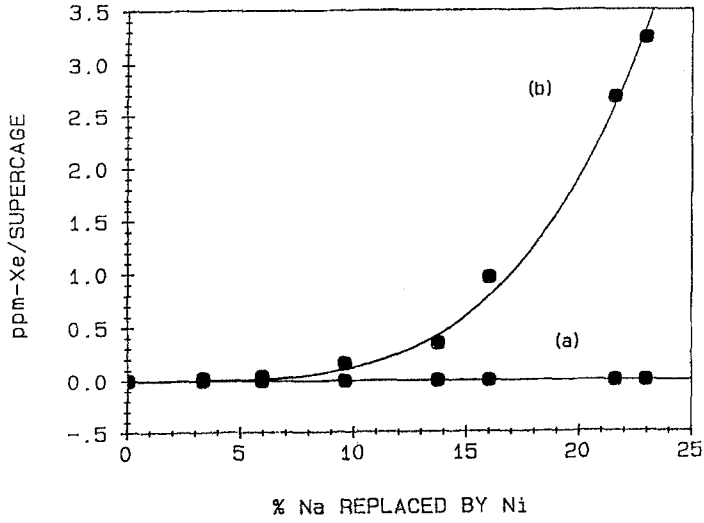

Figure 3. The coefficient, δ_{-1}, of the xenon shift term in inverse density for a series of Ni,Na-Y zeolites as a function of Na ions replaced: (a) samples dehydrated at 298 K; (b) samples dehydrated at 373 K. (After Ref. [35])

Samples dehydrated at 295 K contain a substantial amount of water which most probably sequesters the ions; samples dehydrated at 373 K do contain water, but some form of nickel ion is probably accessible to xenon in these samples. The fact that the inverse-density term appears only for these latter samples, and only at substantial nickel content, indicates that xenon *must* interact directly with some ion of nickel, implying the need for the close contact characteristic of adsorption. It has been found [40] that the xenon-density

dependence of the shift even for Na-Y zeolite has a complex behavior at temperatures below room temperature, in which interactions with ions cause deviations from linearity. Xenon absorbed in a wide variety of other structures has been analyzed by the NMR method: ZSM-5, ZSM-11, L, Z, silicalite [41], mordenite [42], omega and ferrierite [43], beta [44], rho [45], and a silicoalumino-phosphate molecular sieve, SAPO-37 [46].

A Y zeolite structure with platinum ions present gives an even more complex result [47]. For xenon in a Y zeolite containing platinum as well as sodium, the NMR shift depends inversely on the xenon density, showing that the inverse term dominates in these materials. The authors attribute the large shift to electron transfer from xenon to the metal, with structures like $Pt\text{-}Xe^{+}$ contributing to the structure of the chemisorbed complex [47,48]. Similarly, NMR shifts of xenon gas sorbed in platinized aluminas show effects of interaction with the platinum particles [49].

From a practical point of view, xenon NMR experiments on such materials [47] provide an analytical tool to discriminate various regions in the sample. In Pt,Na-Y zeolites in which hydrogen is co-adsorbed with xenon, the xenon NMR spectrum contains several lines. By investigation of the relative intensities of these lines as a function of hydrogen content, Ito and Fraissard [47] demonstrate that each line corresponds to xenon in a region consisiting of platinum particles containing a specific number of hydrogen atoms. Thus, the xenon NMR experiment reports on the inhomogeneous distribution of hydrogen on metal particles. In further experiments using CO as a co-adsorbate, they [47] also show that xenon NMR is sensitive to the distribution of CO on platinum particles. By studying how the spectra change as a function of heat treatment, the authors show that adsorption of CO at 298 K is non-uniform, with CO adsorbing in the region where it first contacts the metal. Heating to 573 K redistributes the CO, which is again detected by a change in the spectrum of xenon co-adsorbed with the CO. Thus, xenon NMR can be used to investigate the distribution of hydrogen and CO in metal-containing zeolites, if the inhomogeneities are larger than the region over which xenon travels (and hence averages the shift).

Processes such as reduction change the ionic composition and the ion positions in a zeolite. These changes may be detected by the effects of the ions on the NMR properties of xenon absorbed in the material [33,34]. For example, as nickel in a Ni,Na-Y zeolite is reduced by treatment with hydrogen, the spectrum of co-adsorbed xenon shows evidence of an inhomogeneous distribution of xenon environments, with two positions becoming particularly prominent. One of these lines is similar in position to that of xenon absorbed in a Na- or H-Y zeolite. This line is not affected by the extent of reduction, whereas the second one is. At sufficiently high reduction temperature (643 K), only the first line is observed, although it is quite broad compared to uniform H-Y zeolites. This observation is consistent with the reduction of nickel ion by replacement with a proton and removal of the nickel from the supercage, most likely moving to the surfaces of the zeolite particles. Upon re-oxidation at high temperature, the line narrows but retains its position, suggesting that the re-oxidation process has made the magnetic environment of xenon more uniform in these particles, but it does not return the material to the state it had before reduction.

Xenon NMR of the absorbed gas is sensitive to differences in the structure of the zeolite in certain cases [50]. While the dependence on xenon density is slightly different from one

zeolite structure to another, the most striking difference is the variation of the wall term, δ_{wall}, with the structure. Demarquay and Fraissard [51] assume this variation with structure results from change in the collision frequency with structure. They define a mean-free-path in the structure that describes the exchange of a xenon atom between a site on the surface of the pore and a site in the void volume of the pore. From this simple picture, they deduce that the wall term depends on this mean-free-path by the following simple relation:

$$\delta_{wall} = \frac{\delta_a}{1 + \lambda/a} \tag{23}$$

where δ_a is a shift determined by the wall adsorption, λ is the mean-free-path in the structure, and a is a coefficient characteristic of the adsorption site [37].

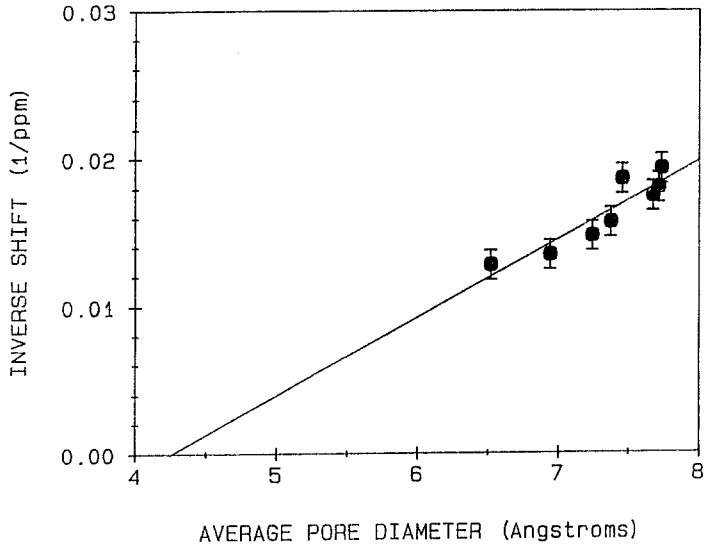

Figure 4. Dependence of $1/\delta_{wall}$ on dynamic pore diameter for a series of dehydrated zeolites, showing that this parameter obeys a relation similar to Equation (9). (After reference [52])

The data of Figure 4 compare $1/\delta_{wall}$ with average dynamic pore diameter for xenon absorbed in several partially dealuminated zeolites [52]. This has the form of the Demarquay-Fraissard equation, if we make the assumption that mean free path and dynamic pore diameter are linearly related. Interestingly, the extrapolation to infinite shift

gives a dynamic pore diameter of 4.3 Å for a pore just large enough to accommodate a xenon atom, close to the accepted van der Waals diameter of the xenon atom of 4.4 Å.

Derouane and Nagy [53] propose an alternative model to predict the dependence of δ_{wall} on structure. In this static picture, the shift results from van der Waals interactions between the adsorbed xenon and oxygen anions in the curved surface of the zeolite pore that produce a paramagnetic contribution to the shift proportional to the interaction energy. The variation of the van der Waals interaction energy with distance to the wall produces a preferred adsorption position [54]. Indeed, the energy at the center of the pore is predicted to be higher than that adjacent to the pore surface, similar to the Ripmeester-Ratcliffe model. Changes in the size of the pore result in a change in position of xenon relative to the pore wall and a concommitant change in average shift detected as a dependence of δ_{wall} on structure. This picture is static, but the fact that positions near the wall are more favored than those near the center of the pore indicates that δ_{wall} is determined by adsorption effects. Since diffusion in these structures carries a xenon atom to thousands of supercages and sites within a supercage during the acquisition of an NMR spectrum [55,56], δ_{wall} surely represents a Boltzmann average over all positions available to xenon.

The density-independent term in the xenon shift, usually ascribed to the effects of the walls, may also reflect changes in the magnetic environment [35]. For example, the exchange of nickel ions for sodium ions shifts the resonance an amount proportional to the amount of nickel [35]. The variation of the shift with nickel concentration was attributed to a variation of the magnetic susceptibility of the sample.

Another application of xenon NMR as a structural probe is the dependence of the shift on calcium content in dehydrated Ca,Na-A zeolites [57]. The shifts extrapolated to the low-uptake limit are linear in the calcium concentration up to 4.5 - 5.0 calcium ions per unit cell. For more than 5.0 Ca^{2+}/unit cell, the shift is constant. This is evidence for different siting of calcium ions. The first 4 or 5 are accessible to xenon in the α-cage, but the additional ions are inaccessible to xenon and thus are unable to influence the shift. This observation is consistent with an X-ray structure of a $Na_{0.4}Ca_{5.2}$-A zeolite [58], in which four calcium ions are found to project into the α-cage and the remaining calcium ion is sequestered in the sodalite cage.

Another experimental effect is seen in the dependence of the xenon shift on the amount of water in a Na-Y zeolite [59]. δ_0 [= δ_{wall} + $\delta_{adsorbate}$] and δ_1 are both affected by the presence of water. δ_0 ranges from 58 ppm for "completely" dehydrated Na-Y zeolite to 158 ppm for a zeolite at 85% of saturated water content. (At water contents above 85% of saturation, the xenon uptake is so low that the resonance intensity is below the detection limit of the spectrometer.) The xenon NMR spectrum depends not only on the water content, but hydration history. Absorption of water produces an inhomogeneous distribution of xenon environments (interpreted as two different regions), whereas desorption produces an apparently uniform xenon environment. δ_0 is independent of water content for concentrations less than 15% of saturation and δ_1 is independent of water content below 40% of saturation. One of the two environments obtained upon adsorption has NMR properties identical to that obtained by desorption, from which the authors conclude that adsorption results in inhomgeneous distributions of water.

Absorption of organic molecules in Na-Y zeolite has effects similar to water on the NMR parameters of co-adsorbed xenon [60]. The results are consistent with a reduction of dynamic pore diameter. As fewer organics are absorbed per cage, the dynamic pore diameter calculated from Equation 23 increases. In addition, the sorption of xenon is observed to saturate at lower pressure when co-adsorbed with organics, an observation consistent with a smaller volume of the supercage. Given that a number of mechanisms may affect the density-independent shift of xenon [35,53], such calculations of dynamic pore diameters should be viewed with caution, particularly if other factors change from sample to sample, but they provide a convenient means to parameterize trends.

One of the more interesting uses of xenon NMR spectroscopy has been the study of materials deposited in the pores of zeolites during the course of a reaction. The quintessential example of this application is the investigation of Y zeolites fouled by the deposition of coke [61]. The deposition of coke changes the pore structure into which xenon is absorbed, affecting the xenon NMR spectroscopy. For some samples, xenon NMR indicates two regions into which xenon absorbed - attributable to pores in the zeolite and to mesopores in the external coke. For the xenon in zeolite pores, the increase in δ_{wall} with coking shows that coke alters the pore structure, estimated in this case from the dependence of δ_0 on the van der Waals interaction energy [53]. The drastic change in δ_1 with coking was interpreted as a change in the void volume per gram of catalyst available to xenon after coking. The shift of the resonance line attributable to xenon in mesopores gave an estimated pore diameter greater than 25 Å. The broadness of the resonance attributable to xenon in the zeolite pores indicates a distribution of environments.

Tsiao et al. [62] used the same technique to investigate acidification of sites in ZSM-5 with various sterically hindered agents. After acidification, the catalysts were coked from 2-butene and examined by xenon NMR spectroscopy of the absorbed gas. The xenon NMR results suggested that the structure of the pores in which the gas absorbed is only slightly changed when acidification is performed with an agent too bulky to enter the channels of the ZSM-5. When a smaller acidifying agent is used, the xenon NMR spectra reveal a channel structure totally altered by the deposition of coke. Significant amounts of internal volume are blocked in this latter treatment which directly affects the NMR spectroscopy of the sorbed xenon.

In a similar system, Tsiao and Botto [63] have investigated xenon absorbed in coal; the xenon NMR spectra were interpreted as evidence for regions with pores of several different sizes in the coal. Conner et al. [64] have investigated the NMR spectroscopy of xenon in pores created by compression of nonporous silica spheres; the mesopore structure being created by agglomeration of the spheres under pressure. The xenon NMR shifts are reasonably independent of the xenon pressure and are interpreted in terms of rapid exchange between sites on the surface of the silica particles and the gas phase trapped between the spheres. It is puzzling that the observed shifts, ranging from 40 ppm to 100 ppm, are comparable to the resonances of xenon in microporous zeolites, yet the only pores are substantially larger than in zeolites.

The ability to distinguish macroscopic regions was exploited in early work in which the distribution of CO on a Pt,Na-Y zeolite was investigated with xenon NMR spectroscopy

[47]. Using a quenched-reaction technique with detection via NMR of absorbed xenon, Tsiao et al. [65] estimated the rate constant for the removal of the template molecules from a pentasil zeolite by observing the collapse of a two-peaked spectrum to a single-peak spectrum. However, the spatial resolution is exceedingly coarse-grained and the collapse of the spectrum to a single resonance only indicates that there are no inhomogeneities of an extent larger than the root-mean-square distance a xenon atom travels in the time it takes to acquire an NMR free-induction decay. If one deliberately creates a macroscopic inhomogeneity, it is possible to detect signals from the separate regions and follow the change in NMR shift as the macroscopic inhomogeneity is eliminated by processes such as diffusion of water from a wet to a dry region [66].

Most of the experiments on xenon in zeolites have been performed at temperatures near 298 K. At this temperature, the adsorbed phase in equilibrium with pressures of xenon up to 1 atmosphere corresponds to densities up to about 100 - 150 amagats, a density 1/3 to 1/2 that of liquid xenon. For Y zeolites, this upper limit corresponds to 3 - 4 xenon atoms per supercage. One can increase the absorption of xenon by performing the spectroscopy at much lower temperatures, as demonstrated by Cheung and coworkers [37,67]. Under these conditions, one can essentially achieve packing of xenon at liquid densities in the void volume of the zeolite. The resulting NMR spectra of adsorbed xenon at these low temperatures exhibit line shifts that depend on the uptake. There are changes in the shift-versus-uptake curve that correspond to the transition from a dense gas to a liquid-like phase in the pores of the zeolite. The form of the chemical-shift-versus-uptake is similar to the adsorption isotherm, suggesting that the change in xenon shift mirrors the change in density. Changes in xenon linewidth suggest that exchange is occurring in these systems, even at rather low temperatures.

4. Deuterium-Containing Aromatics in Zeolites

Understanding the structure and reactivity of organic molecules in catalysts is essential to characterizing heterogeneous catalysis [68]. Thus, a great deal of effort has been expended in analyzing them with spectroscopy, particularly NMR spectroscopy [69]. In addressing aromatic materials absorbed in zeolites, extensive studies have given considerable information about site distributions and dynamics of benzene in zeolite pores [70,71,72] . At low loadings, benzene seems to be partitioned between a window site and a cation site, where it is bound primarily through its π-cloud. Little is known of the behavior of larger aromatic molecules absorbed in zeolites. In our laboratory, we have concentrated on study of phenanthrene-d_{10} (with a long axis of ~9.2 Å), whose size precludes its attachment at the window site in X- and Y-zeolites.

The ^2H NMR spectrum of polycrystalline phenanthrene-d_{10} is a Pake doublet with a splitting between the peak maxima of 128 kHz. This splitting is smaller than the accepted value for an aromatic C-D bond (138 kHz) [73] and results from a slight asymmetry of the electric-field gradient tensor. The spectrum can be simulated with an asymmetry parameter, η, of 0.057 and a quadrupole coupling constant of 179($\pm$1) kHz.

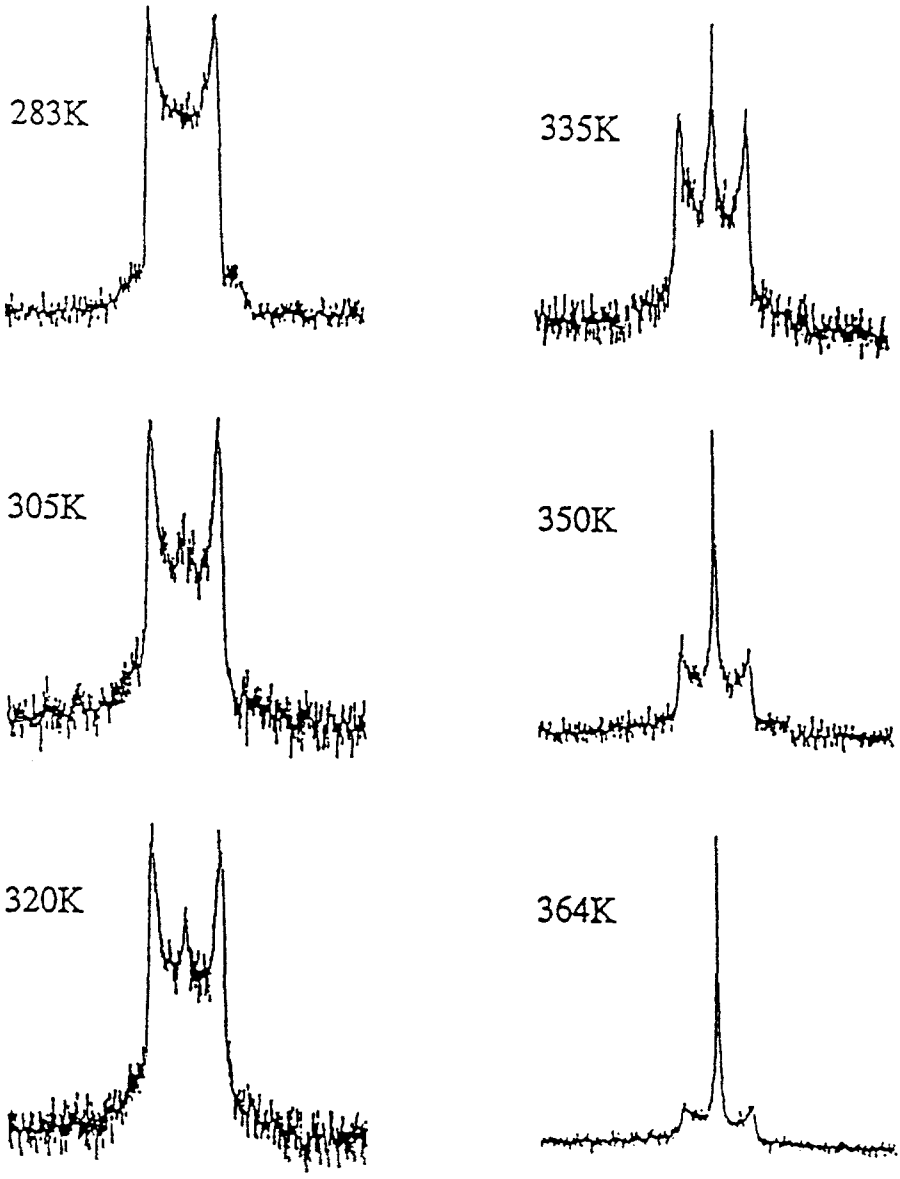

Figure 5. Temperature dependent ^2H NMR spectra of phenanthrene-d_{10} included in K-X zeolite. Each two-component spectrum contains a Lorentzian line superimposed upon a static Pake pattern.

The spectra of phenanthrene-d_{10} in Na- and Cs-X zeolites and Cs-Y zeolite have the same general appearance as those of phenanthrene-d_{10} included in K-X (Figure 5). They are composed of a Lorentzian line superimposed on a static Pake pattern with the same splitting as the polycrystalline sample. The relative amounts of narrow and static components in these spectra vary with temperature for every sample. Inversion-recovery experiments performed on phenanthrene-d_{10} in the Na-, K-, and Cs-X zeolites show that the two components of the spectrum have significantly different T_1's and that the relaxation times are in the range of 1 to 100 ms. This observation demonstrates, for these samples, that there are two distinct spin reservoirs with different motional time constants. Since the T_1 values are in the millisecond range, the exchange rate must be less than 1 kHz. For phenanthrene-d_{10} included in Rb-X and Cs-Y zeolites, only a single T_1 is observed across the line, indicating that exchange between the two states in these samples is rapid enough to equilibrate these two spin reservoirs. Phenanthrene-d_{10} in Rb-X zeolite gives a spectrum that cannot be deconvoluted into two distinct sub-spectra. The lack of hysteresis observed in the line-shape, when the temperature is changed, distinguishes this case from that for a distribution of correlation times, where similar line-shapes are obtained [74].

The nature of the two sites in which phenanthrene may exist when absorbed in these faujasites near room temperature may be addressed by ^2H NMR spectroscopy. Virtually no exchange occurs during the quadrupole-echo experiment, and the deconvolution of the observed spectrum into two distinct sub-spectra is justified. In one state, it is solid-like as detected by NMR spectroscopy. In the other, it is rapidly tumbling, effectively averaging the effects of static quadrupolar couplings to zero. We attribute the observed solid-like state to an ion-bound molecule and the motionally-averaged state to a molecule with enough energy to be free of the ion site. Phenanthrene-d_{10} at these two sites undergoes chemical exchange with a rate constant less than 1 kHz in all but the Rb-exchanged sample. Exchange between two sites has also been inferred from the ^2H NMR spectra of pyrene and anthracene [75].

If two states are connected by chemical exchange, then, at any temperature, an equilibrium is established. The equilibrium constant may be determined from the ratio of the integrated intensities of the two spectral components. The temperature dependence of the equilibrium constant may be used to recover the enthalpy and entropy of association to form the ion-molecule complex from the free phenanthrene-d_{10}. ΔH and ΔS for phenanthrene-ion association in these faujasites, as determined from least-squares fits of van't Hoff plots, are given in Table I. These results agree reasonably well with gas-phase measurements for similar ions interacting with aromatics. For example, the enthalpy and entropy of association for phenanthrene in the K-X zeolite compare well with the results for benzene coordinated to a hydrated potassium ion in the gas phase (ΔH = 12.6 kcal/mol; ΔS = 27.6 cal/K·mol) [76].

The binding of the aromatic ring to the cation is expected to be electrostatic. The binding strength will depend on factors like the electric field or charge density at the binding site and the polarizability and geometry of the interaction. As can be seen in Figure 6, a linear relationship is observed between the heat of dissociation of the complex and the cation radius for phenanthrene-d_{10} in the alkaline-earth exchanged faujasites we have investigated.

Table 1. Enthalpies and Entropies of Association for Ion-Phenanthrene-d_{10} Complexes in Faujasites.

Zeolite	-ΔH (kcal/mol)	ΔS (cal/K·mol)
Sodium-X	14.9±3.5	52.5±12
Potassium-X	11.0±1.8	29.9±5.2
Cesium-X	7.9±2.0	22.7±7.0
Cesium-Y	6.2±2.6	20.3±9.0

The errors shown are the 90% confidence interval of the fitted parameter.

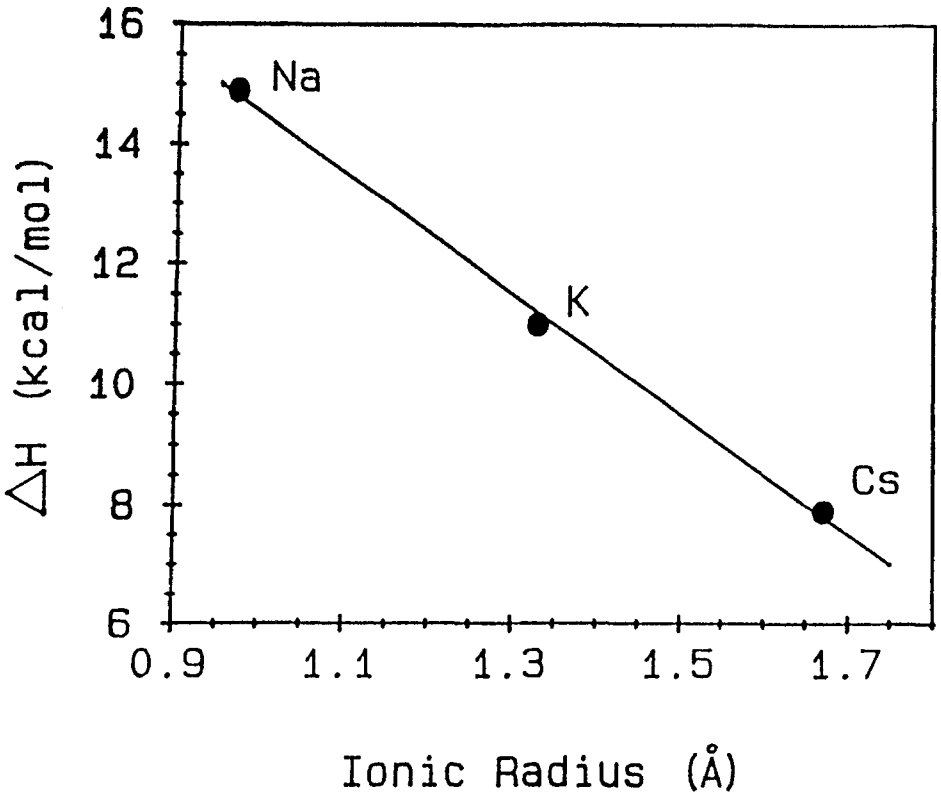

Figure 6. The heat of association versus counterion radius for ion-phenanthrene complexes in X-zeolites.

5. Summary

NMR spectroscopy of xenon is sensitive to the local structure and dynamics of the xenon atom. Because of this sensitivity and the relative ease of performing the ^{129}Xe experiment, xenon is a convenient probe of the state of microporous materials. A number of competing effects influence the shift: interactions with the walls of the micropores, interactions with other xenon atoms, interactions with other absorbed material including direct electrical interactions with ions and the framework, and magnetic effects of ions. Sorting out these various effects can be quite difficult and is a major concern for routine use of xenon NMR spectroscopy as a probe of the environment; it is, in effect, almost too sensitive to many different characteristics of the local environment. Superimposed on these effects is an averaging attendant to the investigation of a highly mobile species. In cases in which one (or a few) effect(s) is (are) dominant, simple models suffice to explain the observed trends in NMR parameters such as the shift. Except for measurements of the diffusion of xenon in the zeolites, few experiments have directly addressed the dynamic state of xenon in these materials.

Acknowledgments

I gratefully acknowledge the financial support of the National Science Foundation (grant CHEM-9013926) during the writing of this review. Students are the lifeblood of an academic research scientist, and I gratefully acknowledge the work of Navin Bansal, Chih-ji Tsiao, Matthew L. Smith, Mark A. Hepp, and Eric Scharpf, without whom this would not have been written.

References

1. R. K Harris, *Nuclear Magnetic Resonance Spectroscopy*, Pitman, London (1983).
2. T. M. Duncan and C. Dybowski, *Surf. Sci. Rep.*, **1**, 157 (1981).
3. J. L. Kaplan and G. Fraenkel, *NMR of Chemically Exchanging Systems*, Academic Press, Boca Raton, Florida (1980).
4. G. J. Schrobilgen, in *NMR and the Periodic Table*, R. K. Harris and B. E. Mann (Eds), Academic Press, New York, Chapter 14 (1978).
5. G. Malli and C. Foroese, *Internat. J. Quantum Chem.*, **1**, 95 (1967).
6. J. A. Pople, W. G. Schneider, and H. J. Bernstein, *High Resolution Nuclear Magnetic Resonance*, McGraw-Hill, New York (1959).
7. D. Brinkman and H. Y. Carr, *Phys. Rev.*, **150**, 174 (1966).
8. (a) R. L. Streever and H. Y. Carr, *Phys. Rev.*, **121**, 20 (1961);
   (b) E. R. Hunt and H. Y. Carr, *Phys. Rev.*, **130**, 2302 (1963);
   (c) W. M. Yen and R. L. Norberg, *Phys. Rev.*, **131**, 269 (1963);

(d) W. W. Warren and R. L. Norberg, *Phys. Rev.*, **148**, 402 (1966).
9. D. Brinkmann, E. Brun, and H. H. Staub, *Helv. Phys. Acta*, **35**, 431 (1962).
10. E. Kanegsberg, B. Pass, and H. Y. Carr, *Phys. Rev. Lett.*, **23**, 572 (1969).
11. A. K. Jameson, C. J. Jameson, and H. S. Gutowsky, *J. Chem. Phys.*, **53**, 2310 (1970).
12. (a) F. J. Adrian, *Phys. Rev. A*, **136**, 980 (1964);
(b) F. J. Adrian, *ibid.*, **138**, 403 (1965).
13. C. J. Jameson, A. K. Jameson, and S. M. Cohen, *J. Chem. Phys.*, **59**, 4540 (1973).
14. (a) A. K. Jameson and C. J. Jameson, *J. Am. Chem. Soc.*, **95**, 8559 (1973);
(b) C. J. Jameson, A. K. Jameson, and S. M. Cohen, *J. Magn. Reson.*, **19**, 385 (1975).
15. A. D. Buckingham and P. A. Kollman, *Mol. Phys.*, **23**, 65 (1972).
16. (a) C. J. Jameson, A. K. Jameson, and S. M. Cohen, *J. Chem. Phys.*, **62**, 4224 (1975);
(b) C. J. Jameson, A. K. Jameson, and S. M. Cohen, *ibid.*, **65**, 3401 (1976);
(c) C. J. Jameson, A. K. Jameson, and S. M. Cohen, *ibid.*, **66**, 5226 (1977).
17. T. R. Stengle, N. V. Reo, and K. L. Williamson, *J. Phys. Chem.*, **85**, 3772 (1981).
18. K. W. Miller, N. V. Reo, A. J. Schoot Uiterkamp, T. R. Stengle, D. P. Stengle, and K. L. Williamson, *Proc. Natl. Acad. Sci.*, **81**, 4946 (1981).
19. F. H. A. Rummens, *Chem. Phys. Lett.*, **31**, 596 (1975).
20. L. Onsager, *J. Am. Chem. Soc.*, **58**, 1486 (1936).
21. B. Linder, *J. Chem. Phys.*, **33**, 668 (1960).
22. J. A. Ripmeester and D. W. Davidson, *J. Mol. Struct.*, **75**, 67 (1981).
23. T. R. Stengle and K. L. Williamson, *Macromolecules*, **20**, 1428 (1987).
24. S. K. Brownstein, J. E. L. Roovers, and D. J. Worsfold, *J. Magn. Reson.*, **26**, 392 (1988).
25. (a) J. A. Ripmeester, *J. Am. Chem. Soc.*, **104**, 289 (1982);
(b) D. Davidson, Y. P. Handa, and J. A. Ripmeester, *J. Phys. Chem.*, **90**, 6549 (1986);
(c) J. A. Ripmeester, J. S. Tse, C. I. Ratcliffe, and B. M. Powell, *Nature*, **325**, 135 (1987).
26. T. Shibanuma, H. Asada, S. Ishi, and T. Matsui, *Jap. J. Appl. Phys.*, **22**, 1656 (1983).
27. G. Neue, *Z. Phys. Chem.*, **152**, 13 (1987).
28. B. C. Gates, J. R. Katzer, and G. C. A. Schuit, *Chemistry of Catalytic Processes*. McGraw-Hill, New York (1979).
29. T. Ito and J. P. Fraissard, *J. Chem. Phys.*, **76**, 5225 (1982).
30. R. C. Weast, (Ed), *Handbook of Chemistry and Physics*, CRC Press, Boca Raton, Florida (1982).
31. J. A. Ripmeester and C. I. Ratcliffe, *J. Phys. Chem.*, **94**, 7652. (1990)

32. W. Heink, J. Kaerger, H. Pfeifer, and F. Stallmach, *J. Am. Chem. Soc.* **112**, 2175 (1990).
33. E. W. Scharpf, R. Crecely, B. C. Gates, and C. Dybowski, *J. Phys. Chem.*, **90**, 9 (1986).
34. J. Fraissard and T. Ito, *Zeolites*, **8**, 350 (1988).
35. N. Bansal and C. Dybowski, *J. Phys. Chem.*, **92**, 2333 (1988).
36. A. Gedeon, J. L. Bonardet, and J. Fraissard, *J. Chim. Phys.*, **85**, 871 (1988).
37. For example, see T. T. P. Cheung, C. M. Fu, and S. J. Wharry, *J. Phys. Chem.*, **92**, 5170 (1988).
38. D. W. Johnson and L. Griffiths, *Zeolites*, **7**, 484 (1987).
39. A. L. R. Bug, *J. Thermophysics*, **10**, 469 (1989).
40. Q. Chen and J. P. Fraissard, Presented at the Fifth International Symposium on Magnetic Resonance in Colloid and Interface Science, Newark, Delaware, 1989.
41. C. J. Tsiao, D. R. Corbin, and C. Dybowski, *J. Phys. Chem.*, **94**, 4195 (1990).
42. J. A. Ripmeester, *J. Magn. Reson.*, **56**, 247 (1984).
43. T. Ito, M. A. Springuel-Huet, and J. P. Fraissard, *Zeolites*, **9**, 68 (1989).
44. R. Benslama, J. P. Fraissard, A. Albizane, F. Fajula, and F. Figueras, *Zeolites*, **8**, 196 (1988).
45. (a) T. Ito and J. P. Fraissard, *Zeolites*, **7**, 554 (1987);
    (b) M. L. Smith, D. R. Corbin, and C. Dybowski, *J. Phys. Chem.*, **97**, 9045 (1993).
46. N. Dumont, T. Ito, and E. G. Derouane, *Appl. Catal.*, **54**, L1 (1989).
47. (a) L. C. deMenorval, J. P. Fraissard, and T. Ito, *J. Chem. Soc., Farad. Trans. I*, **78**, 403 (1982);
    (b) T. Ito, L. C. deMenorval, J. P. Fraissard, and M. Primet, *J. Chem. Soc.,Farad. Trans. I*, **81**, 2855 (1985).
48. (a) B. F. Chmelka, R. Ryoo, S. B. Liu, L. C. deMenorval, C. J. Radke, E. Petersen, and A. Pines, *J. Am. Chem. Soc.*, **110**, 4465 (1988);
    (b) B. F. Chmelka, L. C. deMenorval, R. Csencsits, R. Ryoo, S. B. Liu, C. J. Radke, E. E. Petersen, and A. Pines, *Stud. Surf. Sci. Catal.*, **48**, 269 (1989).
49. M. Boudart, L. C. deMenorval, J. P. Fraissard, and G. P. Valenca, *J. Phys. Chem.*, **92**, 4033 (1988).
50. T. Ito, L. C. deMenorval, E. Guerrier, and J. P. Fraissard, *Chem. Phys. Lett.*, **111**, 271 (1984).
51. J. Demarquay and J. P. Fraissard, *Chem. Phys. Lett.*, **136**, 314 (1987).
52. R. L. Cotterman, D. A. Hickson, S. Cartlidge, C. Dybowski, C. J. Tsiao, and A. F. Venero, *Zeolites*, **11**, 27 (1991).
53. E. G. Derouane and J. B. Nagy, *Chem. Phys. Lett.*, **137**, 341 (1987).
54. E. G. Derouane and M. E. Davis, *J. Mol. Catal.*, **48**, 37 (1988).
55. W. Heink, J. Kaerger, H. Pfeifer and F. Stallmach, *J. Am. Chem. Soc.*, **112**, 2175 (1990).

56. R. Shoemaker and T. M. Apple, *J. Phys. Chem.*, **91**, 4024 (1987).
57. C. J. Tsiao, D. R. Corbin, and C. Dybowski, *J. Phys. Chem.*, **94**, 867 (1990).
58. J. J. Pluth and J. V. Smith, *J. Am. Chem. Soc.*, **195**, 1192 (1983).
59. A. Gedeon, T. Ito and J. P. Fraissard, *Zeolites*, **8**, 376 (1988).
60. (a) R. Ryoo, S. B. Liu, L. C. deMenorval, K. Takegoshi, B. Chmelka, M. Trecoske, and A. Pines, *J. Phys. Chem.*, **91**, 6575 (1987);
    (b) L. C. deMenorval, D. Raftery, S. B. Liu, K. Takegoshi, R. Ryoo, and A. Pines, *ibid.*, **94**, 27 (1990).
61. T. Ito, J. L. Bonardet, J. P. Fraissard, J. B. Nagy, C. Andre, Z. Gabelica, and E. G. Derouane, *Appl. Catal.*, **43**, L5 (1988).
62. C. J. Tsiao, C. Dybowski, A. M. Gaffney, and J. Sofranko, *J. Catal.*, **128**, 520 (1991).
63. C. J. Tsiao and R. Botto, personal communication.
64. W. C. Conner, E. L. Weist, T. Ito, and J. P. Fraissard, *J. Phys. Chem.*, **93**, 4138 (1989).
65. C. J. Tsiao, C. Dybowski, D. Walker, V. Durante, and D. R. Corbin, *Langmuir*, **4**, 1219 (1988).
66. N. Bansal and C. Dybowski, *J. Magn. Reson.*, **89**, 21 (1990).
67. (a) T. T. P. Cheung and C. M. Fu, *J. Phys. Chem.*, **93**, 3740 (1989);
    (b) T. T. P. Cheung, *J. Phys. Chem.*, **94**, 376 (1990).
68. A. de Mallmann, S. Dwizigaj, and D. Barthomeuf, in *Zeolites, Facts, Figures and Future*, P. A. Jacobs and R. A. van Santen, (Eds), Elsevier, Amsterdam, p 935 (1989).
69. H. Pfeifer, W. Meiler, and D. Deininger, *Ann. Rep. NMR Spectrosc.*, **15**, 291 (1983).
70. M. Primet, E. Garbowski, M. Mathieu, and B. Imelik, *J. Chem. Soc., Faraday Trans. 1*, **76**, 1942 (1990).
71. H. Lechert and K. Wittern, *Ber. Bunsenges. Phys. Chem.*, **82**, 1054 (1978).
72. A. N. Fitch, H. Jobic, and A. Renouprez, *J. Chem. Soc., Chem. Commun.*, 284 (1985).
73. J. H. Ok, R. R. Vold, R. L. Vold, and M. C. Etter, *J. Phys. Chem.*, **93**, 7618 (1989).
74. H. A. Riesing, J. K. Thompson, and J. J. Krebs, *J. Phys. Chem.*, **68**, 1621 (1964).
75. Mark A. Hepp, University of Delaware, personal communication
76. R. G. Keesee and A. W. Castleman, *J. Phys. Chem. Ref. Data*, **15**, 1011 (1986).

Abstract. The investigation of xenon and large aromatic molecules adsorbed in zeolitic materials using NMR spectroscopy is discussed. The results suggest a system in which the molecules are often exchanging among adsorption sites. Careful analysis of the spectroscopic results allow one to determine parameters of the magnetic properties of the adsorption sites, as well as factors affecting the exchange.